

The effect of spin exchange interaction on protein structural stability – **Supplementary Information**

Hadar Manis Levy,¹⁺ Avi Schneider,¹⁺ Satyam Tiwari,² Hagit Zer,³ Shira Yochelis,¹ Pierre Goloubinoff,^{*2} Nir Keren^{*3} and Yossi Paltiel^{*1}

¹Applied Physics Department, the Hebrew University of Jerusalem, Jerusalem 91904, Israel

²Department of Plant Molecular Biology, Faculty of Biology and Medicine, University of Lausanne, CH-1015 Lausanne, Switzerland.

³Department of Plant and Environmental Sciences, The Alexander Silberman Institute of Life Sciences, The Hebrew University of Jerusalem, Jerusalem 91904, Israel

Equal contribution +

Corresponding authors: Pierre Goloubinoff,* Nir Keren,* Yossi Paltiel*

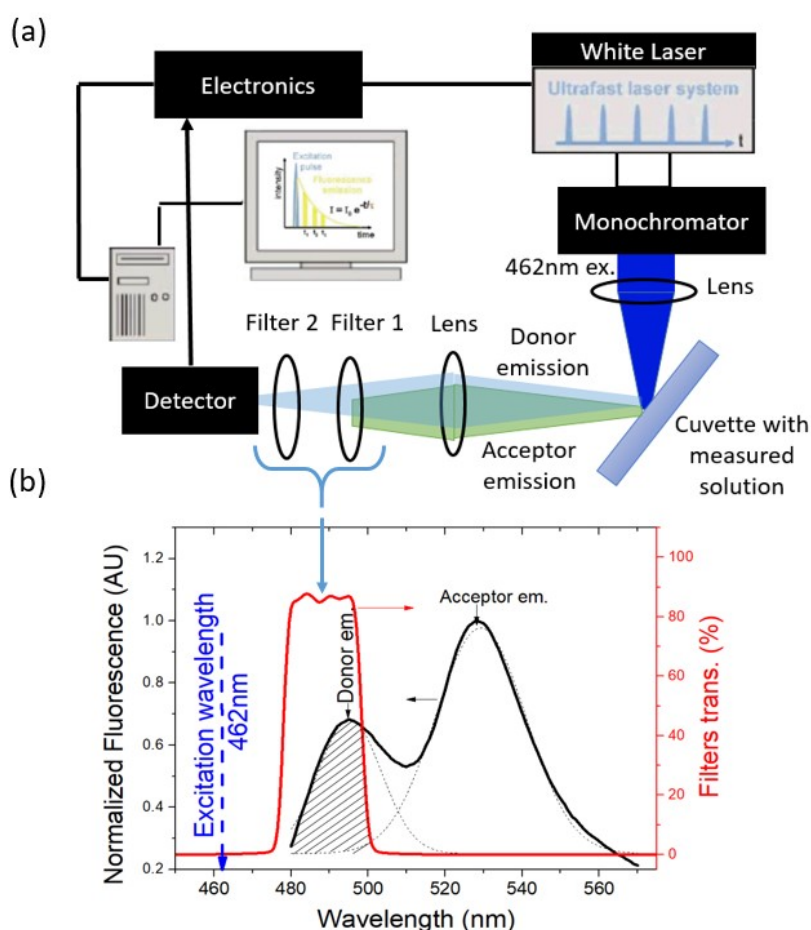


Figure S1 : (a) Fluorescence lifetime measurement set-up. Excited pulsed beam at a wavelength of 462nm was generated and focused on the measured solution by an ultra-fast white light laser followed by a monochromator. The emitted light from both the donor and acceptor chromophores in the solution was collected and focused on the detector. By using a combination of high and low pass filters (Filter 1 and 2) both the acceptor emission and the excitation beam were eliminated. The pulsed excitation beam and the detector were temporally synchronized in order to create the measurement curves. (b) A typical fluorescence spectrum of the MLucV protein solution (black) showing both the donor and acceptor peaks. The transmission spectrum of the two filters (red) shows the range of

wavelengths that were detected in the experiment, emphasized by the dashed area to include only the donor emission.

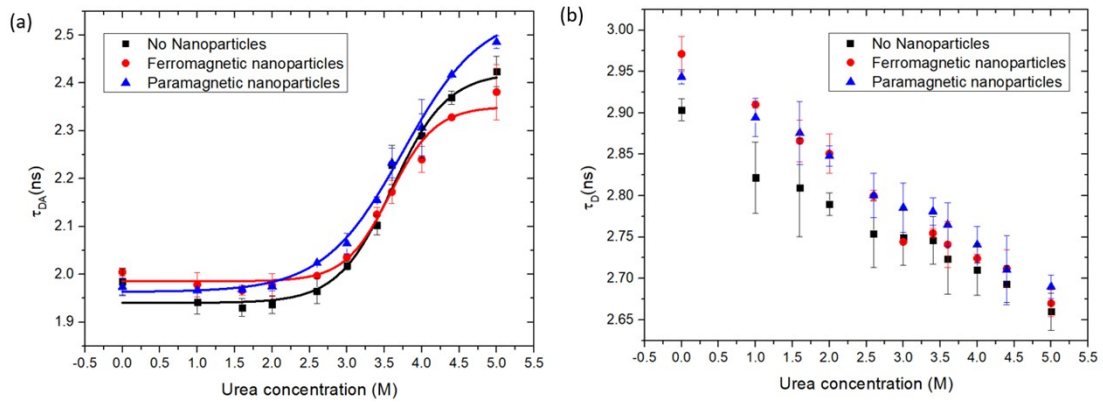


Figure S 2: Donor lifetime measurements in the presence (a) and absence (b) of acceptor as a function of urea concentration for MBarnaseV proteins associated with either ferromagnetic (red), paramagnetic (blue) or no nanoparticles (black) as a reference.

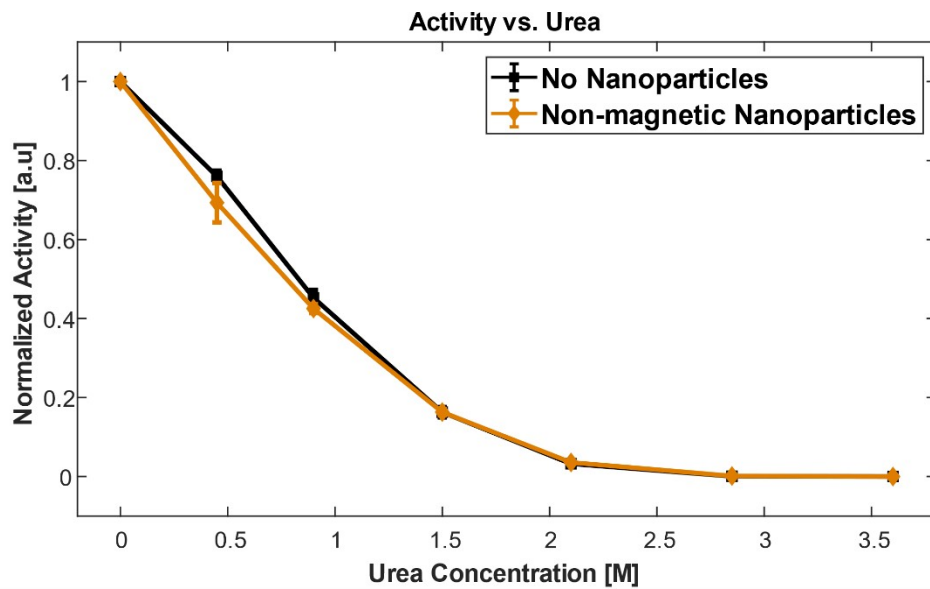


Figure S 3: Activity as a function of Urea concentration for Luciferase proteins (native without chromophores) with either non-magnetic Silicon Titanium oxide nanoparticles (orange/brown) or no nanoparticles at all (black).

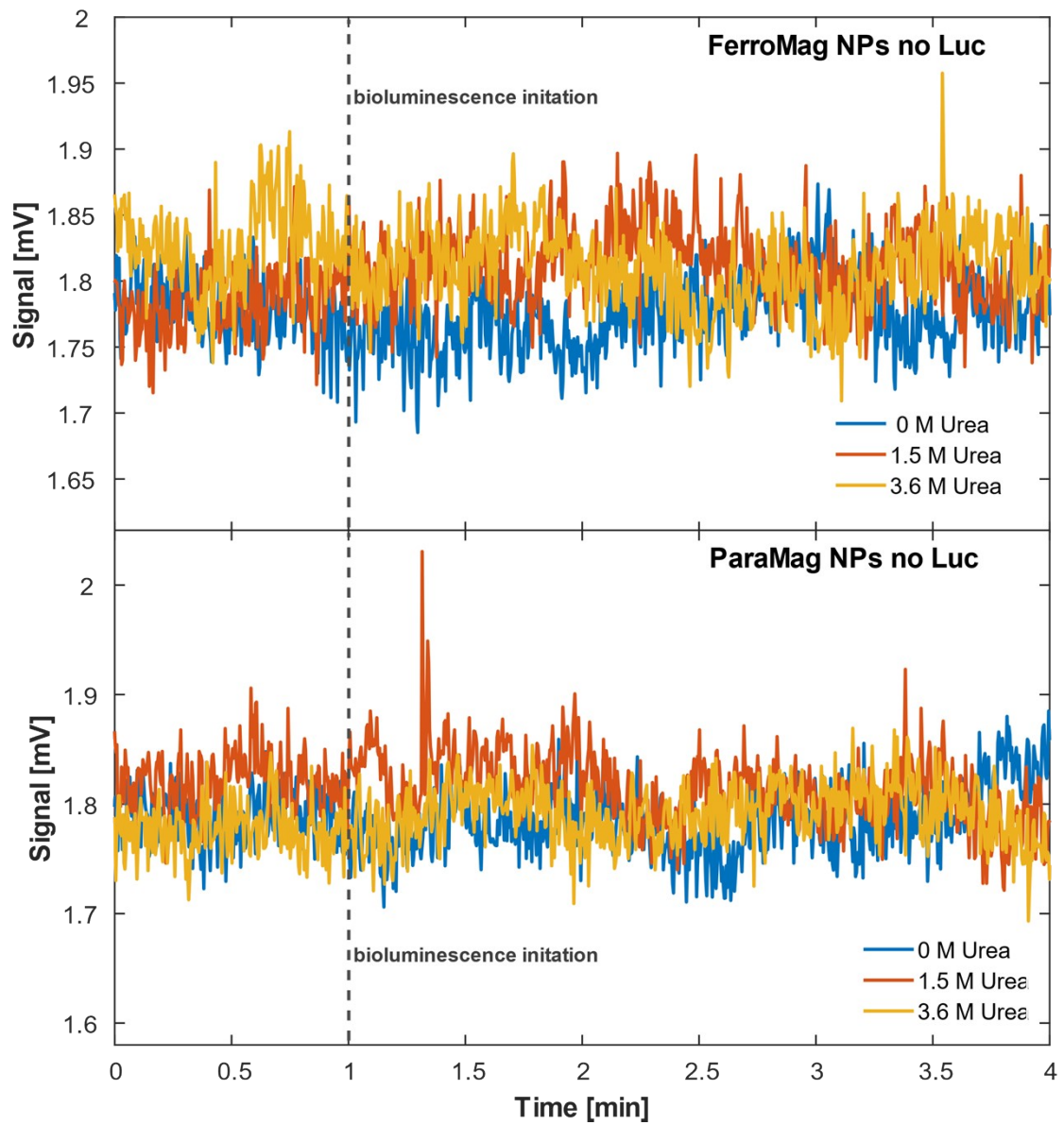


Figure S 4: Activity as a function of Urea concentration for both types of magnetic nanoparticles with no proteins.

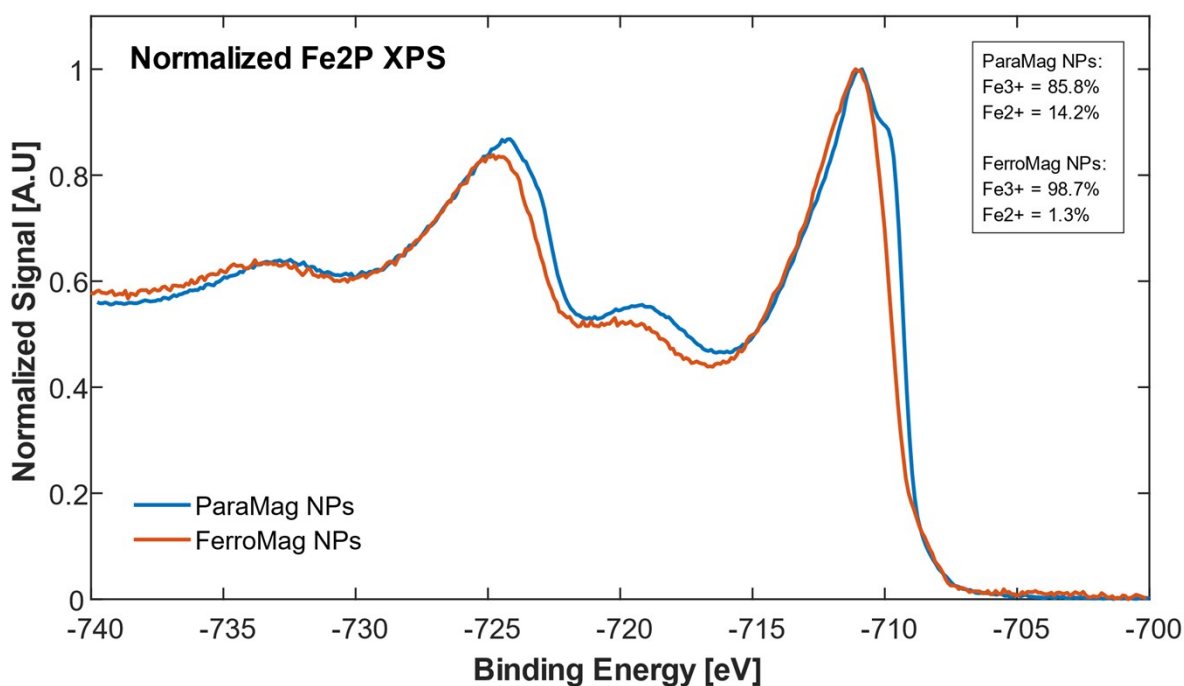


Figure S 5: XPS measurement of the Fe2p orbital for both the Ferromagnetic (orange) and Paramagnetic (Blue) nanoparticles. Inset box: Calculated percentages of Fe2+ and Fe3+ for both types of nanoparticles.

FerroMag NPs:	
element	atomic conc.
O	71.6%
Fe	26.4%
Ba	1.6%
In	0.4%

Table S 1: XPS-calculated atomic concentrations of the elements in the Ferromagnetic nanoparticles.

Surface area (nm ²)	Range	Average
Ferromagnetic Nanoplatelets	314-8796	4555
Paramagnetic Nanorods	1414-6912	4163

Table S 2: Estimated range and average surface areas of the Paramagnetic and Ferromagnetic nanoparticles. The nanoparticle surface area is calculated using a cylinder surface area formula and the particle size range based on electron microscope images. The average value is calculated assuming a symmetrical size distribution.

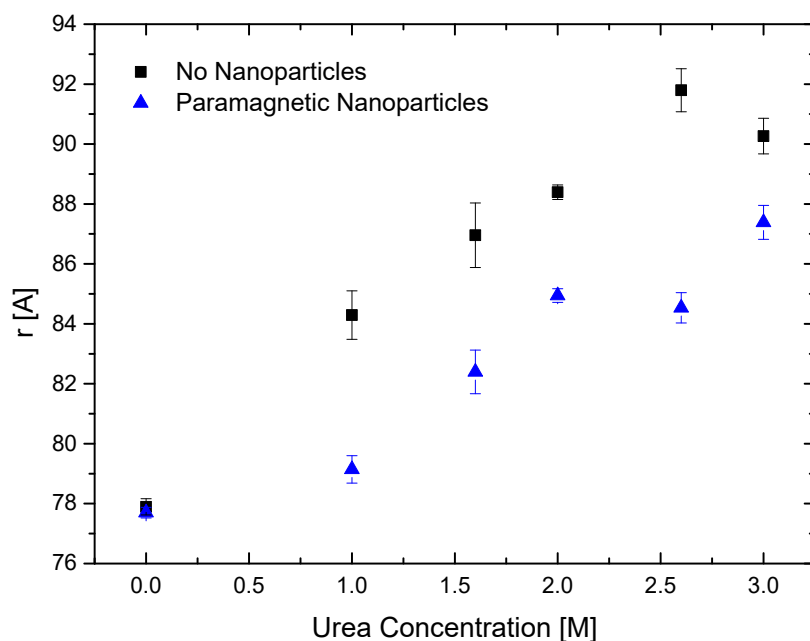


Figure S 6: Average distance between donor and acceptor chromophores as a function of urea concentration for a Luciferase enzyme implanted with the mTFP1 and Venus chromophores at its termini (MLucV) with and without adsorption to paramagnetic nanoparticles.

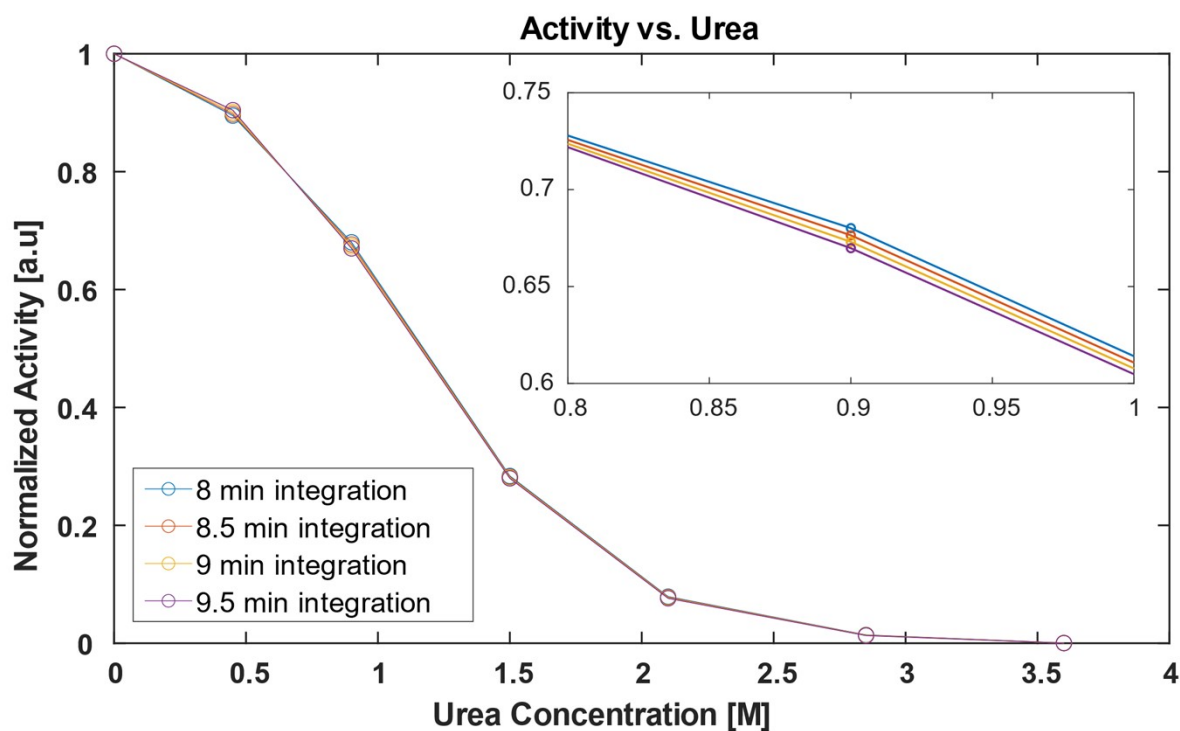


Figure S 7: 'Activity as function of urea concentration' curves for all four integration time intervals (8, 8.5, 9 and 9.5 minutes) of a typical no-nanoparticles measurement. Inset: enlarged section of the main graph around the 0.9 M urea point. The axis units in the inset are identical to those of the main graph.